

## 200 A GeV Au+Au collisions serve a nearly perfect quark-gluon liquid

Huichao Song,<sup>1,2</sup> Steffen A. Bass,<sup>3</sup> Ulrich Heinz,<sup>2</sup> Tetsufumi Hirano,<sup>4,1</sup> and Chun Shen<sup>2</sup>

<sup>1</sup>*Nuclear Science Division, Lawrence Berkeley National Laboratory, Berkeley, California 94720, USA*

<sup>2</sup>*Department of Physics, The Ohio State University, Columbus, Ohio 43210, USA*

<sup>3</sup>*Department of Physics, Duke University, Durham, North Carolina 27708, USA*

<sup>4</sup>*Department of Physics, The University of Tokyo, Tokyo 113-0033, Japan*

(Dated: May 28, 2018)

A new robust method to extract the specific shear viscosity  $(\eta/s)_{\text{QGP}}$  of a Quark-Gluon-Plasma (QGP) at temperatures  $T_c < T \lesssim 2T_c$  from the centrality dependence of the eccentricity-scaled elliptic flow  $v_2/\varepsilon$  measured in ultra-relativistic heavy-ion collisions is presented. Coupling viscous fluid dynamics for the QGP with a microscopic transport model for hadronic freeze-out we find for 200 A GeV Au+Au collisions that  $v_2/\varepsilon$  is a universal function of multiplicity density  $(1/S)(dN_{\text{ch}}/dy)$  that depends only on the viscosity but not on the model used for computing the initial fireball eccentricity  $\varepsilon$ . Comparing with measurements we find  $1 < 4\pi(\eta/s)_{\text{QGP}} < 2.5$  where the uncertainty range is dominated by model uncertainties for the values of  $\varepsilon$  used to normalize the measured  $v_2$ .

PACS numbers: 25.75.-q, 12.38.Mh, 25.75.Ld, 24.10.Nz

Ever since heavy-ion collision experiments at the Relativistic Heavy-Ion Collider (RHIC) demonstrated the creation of color-deconfined Quark-Gluon Plasma (QGP) exhibiting almost ideal fluid dynamical collective behavior [1–3], with viscosity per entropy density  $\eta/s$  approaching the KSS lower bound  $\frac{\eta}{s} \gtrsim \frac{1}{4\pi}$  [4, 5], an accurate extraction of the QGP transport coefficients, especially its shear viscosity  $(\eta/s)_{\text{QGP}}$ , from experimental measurements has been of great interest [6–8]. A small  $\eta/s$  is generally considered to be evidence for the onset of a strongly-coupled deconfined plasma early in the evolution of the collision. RHIC is the first accelerator to provide sufficient beam energy for the QGP to live long enough for flow observables to become sensitive to its intrinsic transport properties. Simulations based on both viscous fluid dynamics and quark-gluon transport theory [6–8] have established that the elliptic flow generated in non-central heavy-ion collisions is particularly sensitive to the shear viscosity  $\eta/s$  of the medium. However, a quantitative extraction of  $(\eta/s)_{\text{QGP}}$  from elliptic flow data requires not only accurate elliptic flow measurements but also a precise knowledge of the theoretical baseline corresponding to zero QGP viscosity. The latter, in turn, requires good control over the fluid’s collective response to anisotropic pressure gradients, and a realistic microscopic description of chemical and kinetic freeze-out during the hadronic stage [9]. A purely hydrodynamic approach that treats both the dense early QGP and dilute late hadron resonance gas phases as viscous fluids not only requires the introduction of two additional parameters, the chemical and kinetic freeze-out temperatures, which must be separately adjusted to experimental data, but ultimately fails [10] because viscous corrections due to hadronic dissipation are large [11] and invalidate a fluid dynamical approach even if it properly accounts for chemical decoupling before kinetic freeze-out [12, 13] and for a strong growth [14] of the specific shear viscosity

$\eta/s$  in the hadronic stage [15].

We here use a newly developed hybrid code (see [10] for details) that couples the relativistic (2+1)-dimensional viscous fluid algorithm VISH2+1 [8] to the microscopic hadronic scattering cascade UrQMD [16] via a Monte Carlo interface [17]. For the QGP fluid we assume constant  $\eta/s$  for  $T_c < T \lesssim 2T_c$  [18]. We switch from a hydrodynamic description of the QGP to UrQMD at temperature  $T_{\text{sw}} = 165$  MeV, adjusted to reproduce the chemical freeze-out temperature measured in RHIC collisions [19] and the highest  $T$  for which we have a valid microscopic description. By giving us full microscopic control, without additional parameters, over the complex hadron kinetic freeze-out our hybrid model opens the door for quantitatively exploring the transport properties of the earlier QGP phase using measured final hadron spectra.

For the hydrodynamic evolution above  $T_{\text{sw}}$  we use the state-of-the-art equation of state (EOS) s95p-PCE based on recent lattice QCD results [13]. The remaining model uncertainties arise mainly from the initial conditions of the hydrodynamic evolution, including the starting time  $\tau_0$  and initial transverse flow velocity. While these cannot be directly measured and require model input, they are tightly constrained by experimental information on the final state [1, 20]. Modeling the QGP as an ideal fluid with  $\eta/s = 0$  and zero initial transverse flow requires an early start at  $\tau_0 = 0.4$  fm/c. Non-zero shear viscosity adds to the transverse pressure [6–8], generating stronger radial flow. The same final flow can then be reached with later starting times, giving the system more time for thermalization. We find [21] that the shapes of the measured pion and proton  $p_T$ -spectra are well reproduced with the following parameter pairs  $(\eta/s, c\tau_0)$ : (0, 0.4 fm), (0.08, 0.6 fm), (0.16, 0.9 fm), and (0.24, 1.2 fm).

For each choice of  $\tau_0$ , the initial energy density is renormalized to yield the same final charged hadron multiplicity  $dN_{\text{ch}}/dy$  in central Au+Au collisions. Its distribution

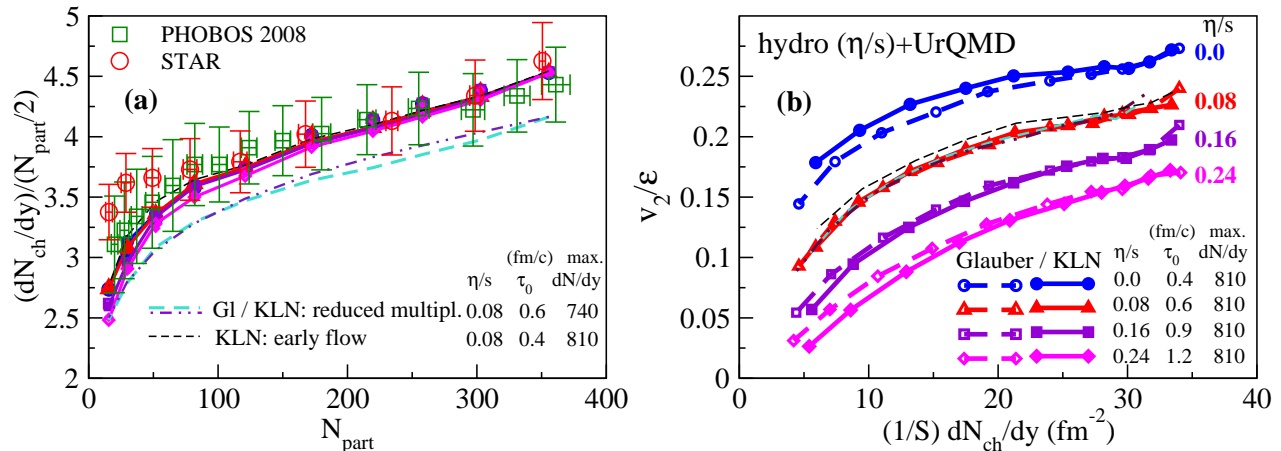


FIG. 1. (Color online) (a) Centrality dependence of the charged hadron rapidity density per participant pair  $(dN_{ch}/dy)/(N_{part}/2)$ . Experimental data are from STAR [33] and PHOBOS [37], using  $dN_{ch}/dy = 1.16 dN_{ch}/d\eta$  for PHOBOS. Theoretical lines are explained in the text. (b) Eccentricity-scaled elliptic flow  $v_2/\epsilon$  as function of multiplicity density  $(1/S)dN_{ch}/dy$ , for different values of  $(\eta/s)_{QGP}$ . Here and in Fig. 2  $v_2$  is integrated with the same cuts as in the STAR data [38]:  $0.15 \text{ GeV}/c < p_T < 2 \text{ GeV}/c$ ,  $|\eta| < 1$ . The overlap area  $S$  is always from the same initial state model as the eccentricity  $\epsilon$  (see text). Note the universality of this theoretical relation, independent of the model used for calculating  $\epsilon$  and  $S$ . Panels (a) and (b) use the same colors and symbols but for clarity not all corresponding curves are shown in both panels.

in the transverse plane is determined (via the EOS) from the initial entropy density distribution  $s(\mathbf{r}, \tau_0; \mathbf{b})$  which we compute, alternatively, from two geometric models discussed below. For the shear viscous pressure tensor we use Navier-Stokes initial conditions [8], noting that the system loses memory after a few relaxation times  $\tau_\pi$  where  $\tau_\pi = \frac{3\eta}{sT} = \mathcal{O}(0.2 \text{ fm}/c)$  [22]. We ignore bulk viscosity due to its small effect on  $p_T$ -spectra and  $v_2$  [23].

The key driver for the elliptic flow generated in the collision is the initial source eccentricity  $\epsilon = \frac{\langle y^2 - x^2 \rangle}{\langle y^2 + x^2 \rangle}$  where  $x$  and  $y$  label the coordinates along the short and long major axes of the fireball in the transverse plane.  $\epsilon$  is computed from the initial entropy density after thermalization [24]. For a quantitative comparison with experiment we account for event-by-event fluctuations of  $\epsilon$  [25] as follows: For each impact parameter, we generate an ensemble of initial entropy density distributions by Monte Carlo (MC) sampling an analytic model of the collision geometry, recentering and rotating each distribution such that its short major axis  $x$  aligns with the direction of the impact parameter. The plane defined by the short major axis and the beam direction ( $x$ - $z$  plane) is called “participant plane”, and the eccentricity using this definition of  $x$  is denoted as  $\epsilon_{part}$ . Superimposing many such events yields a relatively smooth input distribution for hydrodynamic evolution, with an average eccentricity  $\langle \epsilon_{part} \rangle$ . The resulting elliptic flow is interpreted as the event-average  $\langle v_2 \rangle$  for the selected centrality class.

Experimental methods for extracting the elliptic flow [26] typically do not yield  $\langle v_2 \rangle$ . For example, the 2-particle cumulant, denoted by  $v_2\{2\}$ , includes event-by-event flow fluctuations, plus so-called “non-flow” contri-

butions that are outside the purview of hydrodynamics [27, 28]. Fortunately, recent work [28] removed these fluctuation and non-flow contributions from the measured elliptic flow, thereby providing experimental values for  $\langle v_2 \rangle$  that can be normalized by  $\langle \epsilon_{part} \rangle$  for a direct comparison with theory. In the absence of non-flow,  $v_2\{2\} \approx \sqrt{\langle v_2^2 \rangle}$ ; assuming [28]  $\sqrt{\langle v_2^2 \rangle} \approx \frac{\langle v_2 \rangle}{\langle \epsilon_{part} \rangle} \sqrt{\langle \epsilon_{part}^2 \rangle}$  [29], the experimentally determined left side can then again be compared with the theoretically computed right side. We show such a comparison below to check consistency.

To compute the initial entropy density distribution in the transverse plane we use MC versions of the Glauber [31] and fKLN [32] models; for a detailed description of our procedure see [24]. The models are tuned to reproduce the measured collision centrality dependence of  $dN_{ch}/dy$ . Figure 1(a) shows that, for all permissible combinations of  $\tau_0$  and  $\eta/s$  and both MC-Glauber and MC-KLN models for the initial density distribution, the measured centrality dependence of  $dN_{ch}/dy$  is well reproduced. The same holds for the slopes of pion and proton spectra at all centralities [21]. (Following STAR [33],  $dN_{ch}/dy$  does not include charged hyperons and weak decay products.) Two additional curves for initial MC-Glauber and MC-KLN densities with uniformly reduced (by  $\sim 10\%$ ) final multiplicities are shown to demonstrate that, as long as the overall trend is preserved, small differences in  $dN_{ch}/dy$  extracted from STAR, PHOBOS and PHENIX measurements do not influence our conclusions.

Figure 1(b) shows the key theoretical result of the present study: the relation between eccentricity scaled elliptic flow  $v_2/\epsilon$  and multiplicity density  $(1/S)dN_{ch}/dy$  is approximately universal (at least for fixed  $\sqrt{s}$ ), depend-

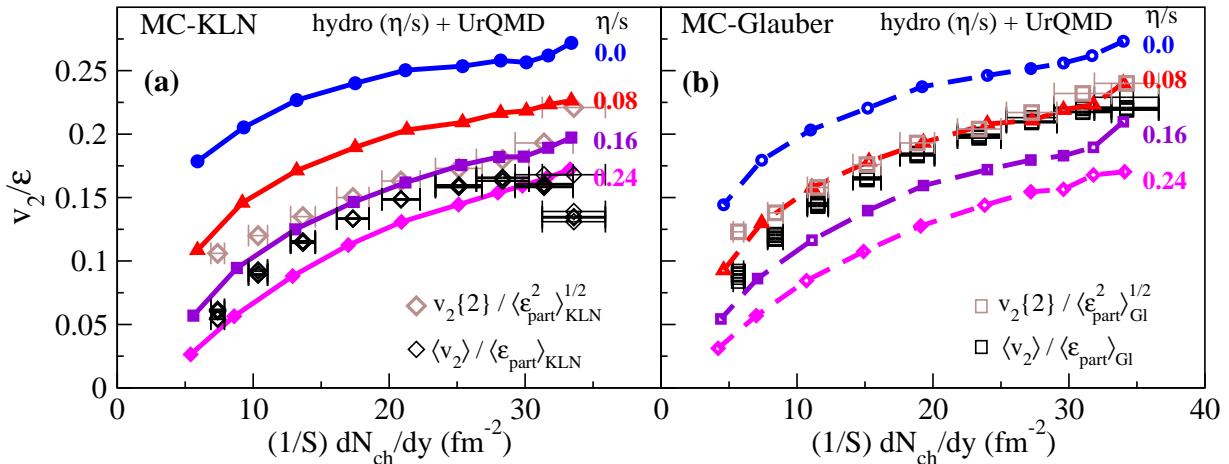


FIG. 2. (Color online) Comparison of the universal  $v_2(\eta/s)/\varepsilon$  vs.  $(1/S)(dN_{\text{ch}}/dy)$  curves from Fig. 1(b) with experimental data for  $\langle v_2 \rangle$  [28],  $v_2\{2\}$  [38], and  $dN_{\text{ch}}/dy$  [33] from the STAR Collaboration. The experimental data used in (a) and (b) are identical, but the normalisation factors  $\langle \varepsilon_{\text{part}} \rangle$  and  $S$  used on the vertical and horizontal axes, as well as the factor  $\langle \varepsilon_{\text{part}}^2 \rangle^{1/2}$  used to normalize the  $v_2\{2\}$  data, are taken from the MC-KLN model in (a) and from the MC-Glauber model in (b). Theoretical curves are from simulations with MC-KLN initial conditions in (a) and with MC-Glauber initial conditions in (b).

ing only on the value of  $\eta/s$  for the QGP but not on any details of the model from which  $\varepsilon$  and  $S = \pi\sqrt{\langle x^2 \rangle \langle y^2 \rangle}$  are computed. To good approximation, switching between initial state models shifts points for a given collision centrality along these universal curves, but not off the lines. For example, reducing the final multiplicity by renormalizing the initial entropy density shifts the points towards the left but also downward because less elliptic flow is created, due to earlier hadronization. The significantly larger  $\langle \varepsilon_{\text{part}} \rangle$  from the KLN model generates more  $v_2$  than for the Glauber model, but the ratio  $v_2/\varepsilon$  is almost unchanged. Slightly larger overlap areas  $S$  for the KLN sources decrease  $(1/S)(dN_{\text{ch}}/dy)$ , but this also decreases the initial entropy density and thus the QGP lifetime, reducing the ratio  $v_2/\varepsilon$ ; the result is a simultaneous shift left and downward. Early flow [34] ( $\tau_0 = 0.4 \text{ fm}/c$  for  $\eta/s = 0.08$ ) increases  $v_2/\varepsilon$  by  $\sim 5\%$ , but the separation between curves corresponding to  $\eta/s$  differing by integer multiples of  $1/(4\pi)$  is much larger. Only in very peripheral collisions is the universality of  $v_2/\varepsilon$  vs.  $(1/S)(dN_{\text{ch}}/dy)$  slightly broken [35].

The clear separation and approximate model-independence of the curves in Fig. 1(b) corresponding to different  $(\eta/s)_{\text{QGP}}$  values suggests that one should be able to extract this parameter from experimental data. However, only  $v_2$  and  $dN_{\text{ch}}/dy$  are experimentally measured whereas the normalization factors  $\varepsilon$  and  $S$  must be taken from a model. Figure 2 shows a comparison of the theoretical curves from Fig. 1(b) with STAR data normalized by eccentricities and overlap areas taken from different initial state models that were all tuned to correctly reproduce the centrality dependence of  $dN_{\text{ch}}/dy$  shown in Fig. 1(a) [39]. Since, for the same model, the eccentricities and overlap areas depend somewhat on

whether they are calculated from the initial energy or entropy density, the same definitions must be used in theory and when normalizing the experimental data.

Both panels of Fig. 2 show the same data, in panel (a) normalized by  $\varepsilon$ ,  $S$  from the MC-KLN model and in (b) with the corresponding values from the MC-Glauber model. The theoretical curves are from the same models as used to normalize the data. The figure shows that comparing apples to apples matters: When comparing the data for  $v_2\{2\}/\langle \varepsilon_{\text{part}}^2 \rangle^{1/2}$  with those for  $\langle v_2 \rangle/\langle \varepsilon_{\text{part}} \rangle$ , the former are seen to lie above the latter, showing that non-flow contributions (which cannot be simulated hydrodynamically) either make a significant contribution to  $v_2\{2\}$  or were overcorrected in  $\langle v_2 \rangle$  [28], especially in peripheral collisions. The extraction of  $\eta/s$  from a comparison with hydrodynamics thus requires careful treatment of both fluctuation and non-flow effects.

The main insight provided by Fig. 2 is that the theoretical curves successfully describe the measured centrality dependence of  $v_2/\varepsilon$ , i.e. its slope as a function of  $dN_{\text{ch}}/dy$ , irrespective of whether the measured elliptic flow is generated by an initial MC-KLN or MC-Glauber distribution. To the best of our knowledge, the hybrid model used here to describe the dynamical evolution of the collision fireball is the first model to achieve this. The magnitude of the source eccentricity (and, to a lesser extent, of the overlap area) disagrees between these two models, and this is the main source of uncertainty for the value for  $(\eta/s)_{\text{QGP}}$  extracted from Fig. 2. Both the Glauber and KLN models come in different flavors, depending on whether the models are used to generate the initial entropy or energy density. We have checked that the versions studied here produce the largest difference in source eccentricity between the models. In this sense

we are confident that Figs. 2(a) and (b) span the realistic range of model uncertainties for  $\varepsilon$  and  $S$ .

We conclude that the QGP shear viscosity for  $T_c < T \lesssim 2T_c$  lies within the range  $1 < 4\pi(\eta/s)_{\text{QGP}} < 2.5$ , with the remaining uncertainty dominated by insufficient theoretical control over the initial source eccentricity  $\varepsilon$ . While this range roughly agrees with the one extracted in [7], the width of the uncertainty band has been solidified by using a more sophisticated dynamical evolution model which eliminates most possible sources of error that the earlier analysis [7] was unable to address. Small bulk viscous effects [23] and proper event-by-event hydrodynamical evolution of fluctuating initial conditions [30] may slightly reduce the ideal fluid dynamical baseline, while pre-equilibrium flow may slightly increase it. Although this should be studied in more quantitative detail, we expect the quoted uncertainty band for  $(\eta/s)_{\text{QGP}}$  to shift, after cancellations, by only a few percent.

We gratefully acknowledge fruitful discussion with P. Huovinen, A. Poskanzer, S. Voloshin, and A. Tang. This work was supported by the U.S. Department of Energy under Grants No. DE-AC02-05CH11231, DE-FG02-05ER41367, DE-SC0004286, and (within the framework of the Jet Collaboration) DE-SC0004104. T.H. acknowledges support through Grant-in-Aid for Scientific Research No. 22740151 and through the Excellent Young Researchers Oversea Visit Program (No. 213383) of the Japan Society for the Promotion of Science.

- 
- [1] U. Heinz and P. F. Kolb, Nucl. Phys. **A702**, 269 (2002).  
 [2] M. Gyulassy, L. McLerran, Nucl. Phys. **A750**, 30 (2005).  
 [3] I. Arsene *et al.*, Nucl. Phys. **A757**, 1 (2005); B. B. Back *et al.*, *ibid.*, p. 28; J. Adams *et al.*, *ibid.*, p. 102; K. Adcox *et al.*, *ibid.*, p. 184.  
 [4] G. Policastro *et al.*, Phys. Rev. Lett. **87**, 081601 (2001); P. K. Kovtun *et al.*, *ibid.* **94**, 111601 (2005).  
 [5] P. Danielewicz, M. Gyulassy, Phys. Rev. D **31**, 53 (1985).  
 [6] D. Molnar and M. Gyulassy, Nucl. Phys. **A697**, 495 (2002); D. Teaney, Phys. Rev. C **68**, 034913 (2003); R. A. Lacey *et al.*, Phys. Rev. Lett. **98**, 092301 (2007); A. Adare *et al.*, *ibid.* **98**, 172301 (2007); H.-J. Drescher *et al.*, Phys. Rev. C **76**, 024905 (2007); K. Dusling and D. Teaney, *ibid.* **77**, 034905 (2008); Z. Xu *et al.*, Phys. Rev. Lett. **101**, 082302 (2008); D. Molnar and P. Huovinen, J. Phys. G **35**, 104125 (2008); A. K. Chaudhuri, *ibid.* **37**, 075011 (2010).  
 [7] P. Romatschke and U. Romatschke, Phys. Rev. Lett. **99**, 172301 (2007); M. Luzum and P. Romatschke, Phys. Rev. C **78**, 034915 (2008).  
 [8] H. Song and U. Heinz, Phys. Lett. **B658**, 279 (2008); Phys. Rev. C **77**, 064901 (2008); *ibid.* **78**, 024902 (2008).  
 [9] H. Song and U. Heinz, J. Phys. G **36**, 064033 (2009).  
 [10] H. Song, S. A. Bass and U. Heinz, Phys. Rev. C **83**, 024912 (2011).  
 [11] T. Hirano *et al.*, Phys. Lett. **B636**, 299 (2006).  
 [12] D. Teaney *et al.*, arXiv:nucl-th/0110037; T. Hirano and K. Tsuda, Phys. Rev. C **66**, 054905 (2002).  
 [13] P. Huovinen and P. Petreczky, Nucl. Phys. **A837**, 26 (2010); C. Shen *et al.*, Phys. Rev. C **82**, 054904 (2010).  
 [14] N. Demir *et al.*, Phys. Rev. Lett. **102**, 172302 (2009); J. Noronha-Hostler *et al.*, *ibid.* **103**, 172302 (2009).  
 [15] C. Shen and U. Heinz, Phys. Rev. C, in press [arXiv:1101.3703].  
 [16] S. A. Bass *et al.*, Prog. Part. Nucl. Phys. **41**, 255 (1998).  
 [17] We here consider only the mid-rapidity region where the approximation of longitudinal boost-invariance is justified. The physics at forward rapidity requires additional study.  
 [18] L. P. Csernai *et al.*, Phys. Rev. Lett. **97**, 152303 (2006).  
 [19] P. Braun-Munzinger *et al.*, Phys. Lett. B **518**, 41 (2001).  
 [20] T. Hirano *et al.*, Phys. Rev. C **77**, 044909 (2008).  
 [21] H. Song *et al.*, arXiv:1101.4638.  
 [22] The choice of QGP shear relaxation time has small to negligible effects on the final spectra and elliptic flow [8].  
 [23] H. Song and U. Heinz, Phys. Rev. C **81**, 024905 (2010).  
 [24] T. Hirano and Y. Nara, Phys. Rev. C **79**, 064904 (2009); T. Hirano *et al.*, *ibid.* **83**, 021902 (2011).  
 [25] M. Miller and R. Snellings, arXiv:nucl-ex/0312008; B. Alver *et al.*, Phys. Rev. Lett. **104**, 142301 (2010).  
 [26] S. A. Voloshin *et al.*, arXiv:0809.2949.  
 [27] B. Alver *et al.*, Phys. Rev. C **77**, 014906 (2008).  
 [28] J. Y. Ollitrault *et al.*, Phys. Rev. C **80**, 014904 (2009).  
 [29] Recent work on event-by-event hydrodynamics [30] suggests that  $\langle v_2^2 \rangle / \langle \varepsilon_{\text{part}}^2 \rangle \lesssim \langle v_2 \rangle^2 / \langle \varepsilon_{\text{part}} \rangle^2$  where the difference is small for the  $p_T$ -integrated elliptic flow studied here but visible in the differential  $v_2(p_T)$  at large  $p_T$ .  
 [30] R. P. G. Andrade *et al.*, Phys. Rev. Lett. **101**, 112301 (2008); H. Petersen and M. Bleicher, Phys. Rev. C **81**, 044906 (2010); H. Holopainen *et al.*, arXiv:1007.0368; H. Petersen *et al.*, Phys. Rev. C **82**, 041901 (2010); B. Schenke *et al.*, Phys. Rev. Lett. **106**, 042301 (2011).  
 [31] M. L. Miller, K. Reygers, S. J. Sanders and P. Steinberg, Ann. Rev. Nucl. Part. Sci. **57**, 205 (2007).  
 [32] H. J. Drescher and Y. Nara, Phys. Rev. C **75**, 034905 (2007); **76**, 041903(R) (2007).  
 [33] B. I. Abelev *et al.*, Phys. Rev. C **79**, 034909 (2009).  
 [34] Some radial and elliptic flow may develop in the pre-equilibrium stage [36]. To mimic such early flow we reduce  $\tau_0$  to 0.4 fm/c here, still marginally fitting the  $p_T$ -spectra.  
 [35] Here we focus on fixed-energy Au+Au collisions at different centralities. Further studies are needed to see if this universality carries over to other collision energies [8, 24].  
 [36] J. Vredevoogd, S. Pratt, Phys. Rev. C **79**, 044915 (2009).  
 [37] B. B. Back *et al.*, Phys. Rev. C **70**, 021902 (2004); B. Alver *et al.*, *ibid.* **80**, 011901 (2009).  
 [38] J. Adams *et al.*, Phys. Rev. C **72**, 014904 (2005).  
 [39] We found this tuning to be an essential ingredient for a meaningful comparison between data and theory.